

## Citation

Li, Z. and Yang, Q. and Chen, W. and Hao, H. and Matenga, C. and Huang, Z. and Fang, R. 2021. Impact response of a novel sandwich structure with Kirigami modified corrugated core. *International Journal of Impact Engineering*. 156: ARTN 103953. <http://doi.org/10.1016/j.ijimpeng.2021.103953>

# 1 Impact response of a novel sandwich structure with 2 Kirigami modified corrugated core

3 Zhejian Li<sup>1</sup>, Qiusong Yang<sup>1</sup>, Wensu Chen<sup>2\*</sup>, Hong Hao<sup>2\*</sup>, Callan Matenga<sup>2</sup>, Zhijie Huang<sup>2, 3</sup>,  
4 Rui Fang<sup>1</sup>

5 <sup>1</sup> *Guangzhou University-Curtin University Joint Research Centre for Structural Monitoring and*  
6 *Protection against Multi-Dynamic Hazards, School of Civil Engineering, Guangzhou University,*  
7 *China*

8 <sup>2</sup>*Center for Infrastructural Monitoring and Protection, School of Civil and Mechanical Engineering,*  
9 *Curtin University, Australia*

10 <sup>3</sup>*Institute of Geotechnical Engineering, Zhejiang University, China*

11 \* Corresponding authors. [wensu.chen@curtin.edu.au](mailto:wensu.chen@curtin.edu.au) (W. Chen), [hong.hao@curtin.edu.au](mailto:hong.hao@curtin.edu.au) (H.  
12 Hao).

## 13 **Abstract**

14 A novel Kirigami modified corrugated core was proposed recently and its superior crushing  
15 performance under static loading was demonstrated. The proposed core is modified from the  
16 conventional corrugated core using Kirigami design, where a portion of the corrugated sheet is  
17 cut and then folded vertically. The vertical fold-ins of Kirigami modified corrugated core  
18 provide extra support and constraints to the adjacent un-folded cell walls, which increase the  
19 crushing resistance of a unit cell up to 10 times as previously studied. However, for a panel  
20 with multiple unit cells, its longitudinal flexural stiffness and impact resistance could be  
21 affected because of the fold-ins. This study investigates its performance and energy absorption  
22 under dynamic crushing through pendulum impact tests. Four configurations of panels,  
23 including laminated flat plate (FL), conventional corrugated (CC), Kirigami modified  
24 corrugated 1 (KC1) and Kirigami modified corrugated 2 (KC2) were tested. Different impact  
25 mass, velocities as well as impacting locations were considered. Impact force and rear face  
26 centre deflection were measured and compared to evaluate the impact performance of the

27 panels. Superior impact resistance was demonstrated for proposed KC panel over CC panel  
28 under all impact scenarios.

29 **Keywords:** Impact; Testing; Kirigami structure; Corrugated core; Sandwich structure

## 30 **1 Introduction**

31 Resilient design of structures is becoming more and more important nowadays. How to protect  
32 structures and quickly recover from severe loading effects such as blast and impact, is a  
33 challenge. Sandwich panel, which often consists of two stiff plates and a light-weight crushable  
34 core, is widely used as protective structures to mitigate the damage from impact or blast.  
35 Sandwich structures of different materials [1, 2] and a variety of core topologies [3-6] have  
36 been extensively investigated under various loading conditions. Out of these topologies,  
37 corrugated core shows characteristics of high specific strength, high shear strength along the  
38 longitudinal direction as well as high flexural strength [7-9]. Owing to its mechanical property,  
39 as well as the relatively simple and low manufacturing cost, the corrugated core has been  
40 widely used in ship building [4, 10] and as protective structures against blast [11, 12] and  
41 impact loads [13, 14].

42 The flatwise compressive strength of the corrugated core is significantly lower than that of the  
43 honeycomb of the same relative density, although its longitudinal shear strength is comparable  
44 with honeycomb [7, 15]. Furthermore, high force at the initial stage of crushing has been  
45 observed under quasi-static loading of corrugated cores made of different materials [7, 8]. High  
46 fluctuations in crushing resistance of multilayer corrugated cores were observed [16] and the  
47 non-uniform behaviour in crushing resistance was also common under higher loading rates [16,  
48 17]. As these crushing characteristics of the corrugated core are not ideal for energy absorption  
49 purposes, numerous modifications on conventional corrugated cores, such as the addition of  
50 foam [18-21], ceramic [22], honeycomb [23], sand [24] and fluid [25] fillers, hierarchical wall

51 [26], graded multilayer via varying geometries [17] or wall thicknesses [27] and double  
52 corrugation [5, 28] etc., have been proposed to improve one or multiple aspects of the  
53 mechanical properties of the conventional corrugated core. These mentioned modifications on  
54 corrugated cores may have some drawbacks, despite the improvements in energy absorption  
55 and crushing resistance. For instance, the addition of fillers could significantly increase the  
56 mass of the light-weighted core as well as the cost, and extra bonding or sealing may be  
57 required depends on the types of fillers. Modified corrugated cores with complex geometries  
58 such as hierarchical walls and double corrugation could be difficult and expensive to fabricate,  
59 and the size of the structure could be limited.

60 A simple Kirigami modification was proposed based on a unit cell of the corrugated core, where  
61 two ends of the cell were cut and folded vertically [29]. This proposed modification introduces  
62 no additional weight to the core and minimal changes to the manufacturing process of the  
63 conventional corrugated cores. The quasi-static and dynamic mechanical properties and  
64 crushing behaviours of the proposed Kirigami corrugated unit cells were studied and compared,  
65 based on flatwise crushing tests and numerical simulations [29]. Due to the additional support  
66 provided by the vertical fold-in and the constraint to the adjacent sidewalls, Kirigami modified  
67 corrugated unit cell increased the average crushing resistance by several times than  
68 conventional corrugated unit cell, and without a distinct initial peak in crushing resistance.  
69 Furthermore, the modified corrugated core became less sensitive to loading rates. However,  
70 the study [29] was conducted under quasi-static crushing on a single unit cell of the corrugated  
71 core with bolted boundary, different to the corrugated panels in most of the applications, which  
72 consist of an array of unit cells. Moreover, in Kirigami modification process, a portion of the  
73 corrugated core is cut and folded vertically, which could lead to a reduction in longitudinal  
74 flexural stiffness of a panel or beam consisting of multiple corrugated unit cells. As some

75 portion of the front surface were folded, the localized frontal impact response of a Kirigami  
76 corrugated sandwich structure can be also affected, depending on the impact location.

77 In this study, the impact resistance of sandwich panels with Kirigami modified corrugated core  
78 was experimentally investigated and compared with the conventional corrugated sandwich  
79 panel and laminated flat plate. The manufacturing feasibility of the proposed modification on  
80 conventional corrugated was testified by including multiple modified unit cells rather than a  
81 single unit cell. The panel specimens were clamped around the boundary and impacted by a  
82 pendulum in the centre. Various impact loads were considered by applying different impact  
83 masses and impact velocities. Two configurations of sandwich panels with Kirigami modified  
84 corrugated core were tested to compare the responses for impacting at the centre of a unit cell  
85 and impacting in-between unit cells. To evaluate the energy absorption of the proposed  
86 Kirigami modified corrugated panels, numerical simulations were carried out for three  
87 sandwich panels under standard impact loads. Impact force time histories and rear plate centre  
88 displacement time histories were recorded and compared to evaluate the impact resistance of  
89 each design under different loading scenarios.

## 90 **2 Specimen geometries and preparation**

### 91 2.1 Specimen geometries

$$c = h \quad (1)$$

$$d = \sqrt{a^2 + h^2} \quad (2)$$

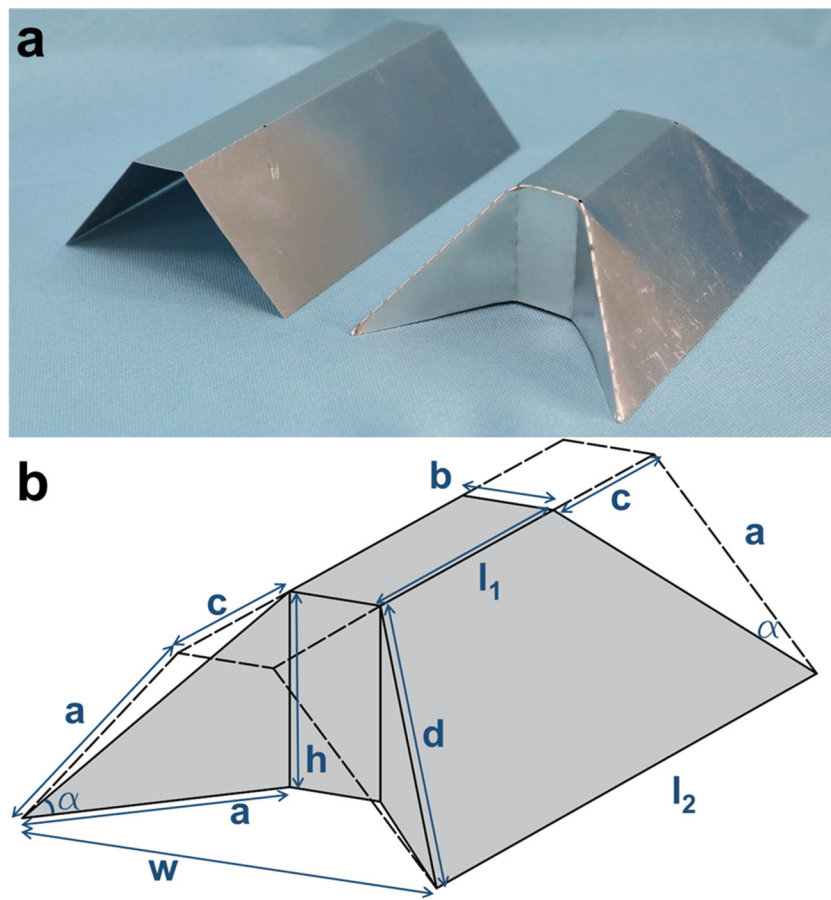
$$\alpha = \text{atan}(h / a) \quad (3)$$

$$w = 2\sqrt{a^2 - h^2} + b \quad (4)$$

$$l_1 = l_2 - 2h \quad (5)$$

92 The proposed Kirigami modification on a unit cell of corrugated core is shown in Figure 1,  
93 where two ends of the corrugated core are folded vertically. The fold-ins provides lateral

94 crushing resistance, as well as constraints to the adjacent unfolded corrugated cell walls. This  
 95 combined effect significantly enhances the energy absorption and the average crushing  
 96 resistance of the corrugated core. Up to 10 times increase in average crushing resistance was  
 97 observed for a Kirigami modified corrugated unit cell [29]. The geometric parameters of a  
 98 Kirigami modified corrugate unit cell are marked out in Figure 1 (b), and the geometries of the  
 99 unit cell are governed by the cell wall width,  $a$ , top width,  $b$ , and cell height,  $h$ . Other parameters  
 100 can be expressed as follows.

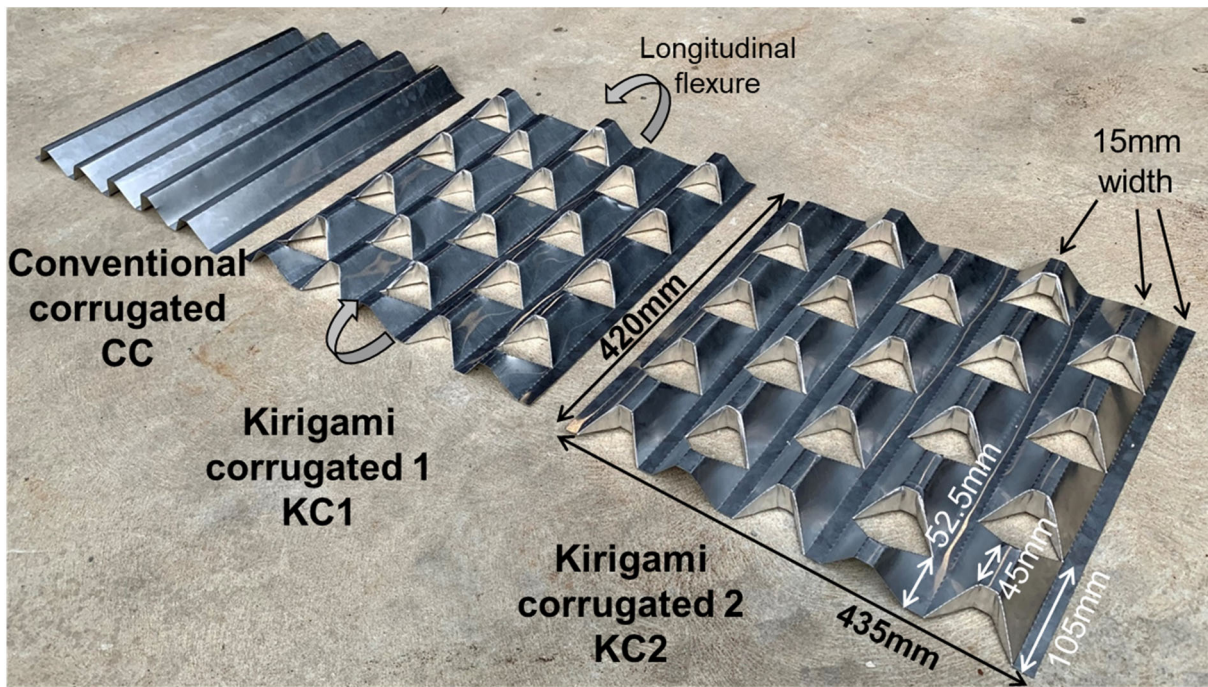


101  
 102 Figure 1. (a) Unit cell of the corrugated core before (L) and after (R) Kirigami modification;  
 103 (b) geometric parameters of a Kirigami modified corrugated unit cell

104 Table 1. Geometric parameters of a Kirigami modified corrugated unit cell

$a$ (mm)	$b$ (mm)	$c$ (mm)	$d$ (mm)	$h$ (mm)	$w$ (mm)	$l_1$ (mm)	$l_2$ (mm)	$\alpha$ (degree)
40	15	30	50	30	67.9	45	105	36.9

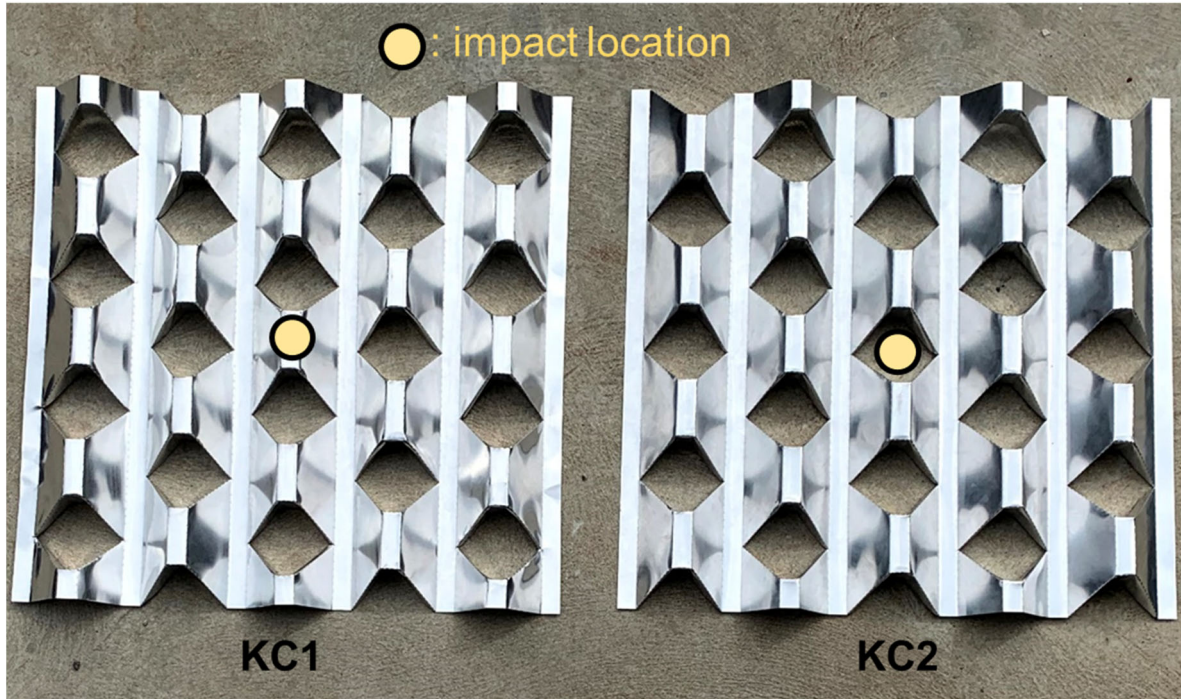
105 The geometric parameters used for the unit cell of Kirigami modified corrugated core are listed  
106 in Table 1. Three configurations of panel cores including one conventional corrugated core,  
107 two Kirigami modified corrugated cores are noted as CC, KC1 and KC2 and shown in Figure  
108 2. The corrugations for all cores were the same, with top width,  $b$ , of 15mm, bottom width,  $w$ ,  
109 of 67.9 mm and sidewall width,  $a$ , of 40 mm. Each core consisted of 5 rows of corrugations,  
110 separated by flat strips with a width of 15 mm as shown in Figure 2. The overall dimension of  
111 the core was around 420×435×30 mm. For Kirigami modified corrugated cores, each row of  
112 the corrugation was made of either 4 complete cells or 3 complete cells plus two halves, as the  
113 cells between adjacent rows were offset by half cell. These half-cell offsets were designed to  
114 minimize the effect of cut-outs on the longitudinal flexural stiffness of the panel.



116 Figure 2. Three configurations of cores: conventional corrugated (CC), Kirigami corrugated 1  
117 (KC1) and Kirigami corrugated (KC2) from left to right

118 As shown in Figure 3, two configurations of Kirigami modified corrugated cores were prepared  
119 to examine the effect of impact location on the performance of proposed sandwich panels with  
120 Kirigami modified corrugated core. The panel with KC2 core configuration was included to  
121 investigate the impact response when the localized impact was on top of a void between two

122 Kirigami corrugated cells. To examine the scenario when an impact was localized between two  
123 adjacent columns of corrugation, back face impact was carried out for all three configurations  
124 of panels, where the panels were flipped and impacted. More information regarding the test is  
125 provided in the next section.



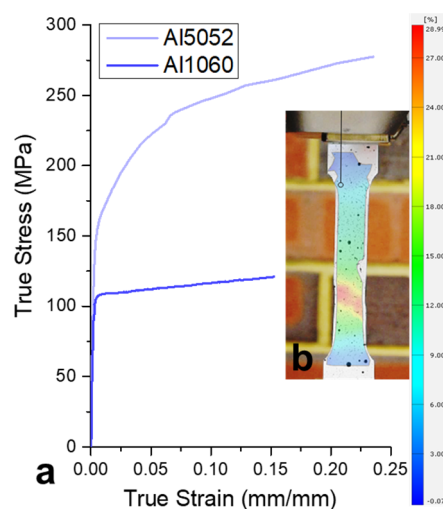
126  
127 Figure 3. Top view of two configurations of Kirigami modified corrugated cores and  
128 approximate impact location for the frontal impact of each panel

## 129 2.2 Specimen preparation and material properties



130  
131 Figure 4. Sandwich panel specimens with three configurations of corrugated cores  
132 The cores were firstly folded from laser-patterned aluminium 1060 sheet with a thickness of  
133 0.26 mm and density of  $2700 \text{ kg/m}^3$ . Each corrugated core was then sandwiched by two 5052  
134 H32 aluminium plates, each with a dimension of  $450 \times 430 \times 2 \text{ mm}$ . The density of 5052 H32

135 aluminium is  $2680 \text{ kg/m}^3$ . The overall dimension of each panel specimen was  $450 \times 430 \times 34$   
136 mm, as all corrugated core had a height of 30 mm. The panels were bonded using a mixture of  
137 epoxy resin and hardener. The epoxy resin has an ultimate tensile strength of 50.5 MPa. A total  
138 of 10 panels with corrugated cores were prepared, including four panels with conventional  
139 corrugated core (CC), four panels with Kirigami corrugated core configuration 1 (KC1), and  
140 two panels with Kirigami corrugated core configuration 2 (KC2), as shown in Figure 4. One  
141 laminated plate with a dimension of  $450 \times 430 \times 4$  mm was also prepared by bonding front and  
142 rear plates without the core. Each core had a relative density of around 1.1% and a mass of  
143 about 0.17 kg. The front and back aluminium plates weigh around 1.04 kg each. The overall  
144 mass of each corrugated panel was about 2.25 kg, and the mass of the laminated plate was 2.08  
145 kg. Tensile tests of aluminium 1060 sheets and aluminium 5052 H32 plates were carried out  
146 under quasi-static loading condition. The yield strength for Aluminium 1060 and 5052 were  
147 measured as 108 MPa and 159 MPa, respectively. Young's modulus of 70 GPa was also  
148 measured for the both aluminium materials. 2D digital image correlation (DIC) technique was  
149 used for measuring the strain of the tensile specimens. The tensile test results are shown in  
150 Figure 5.

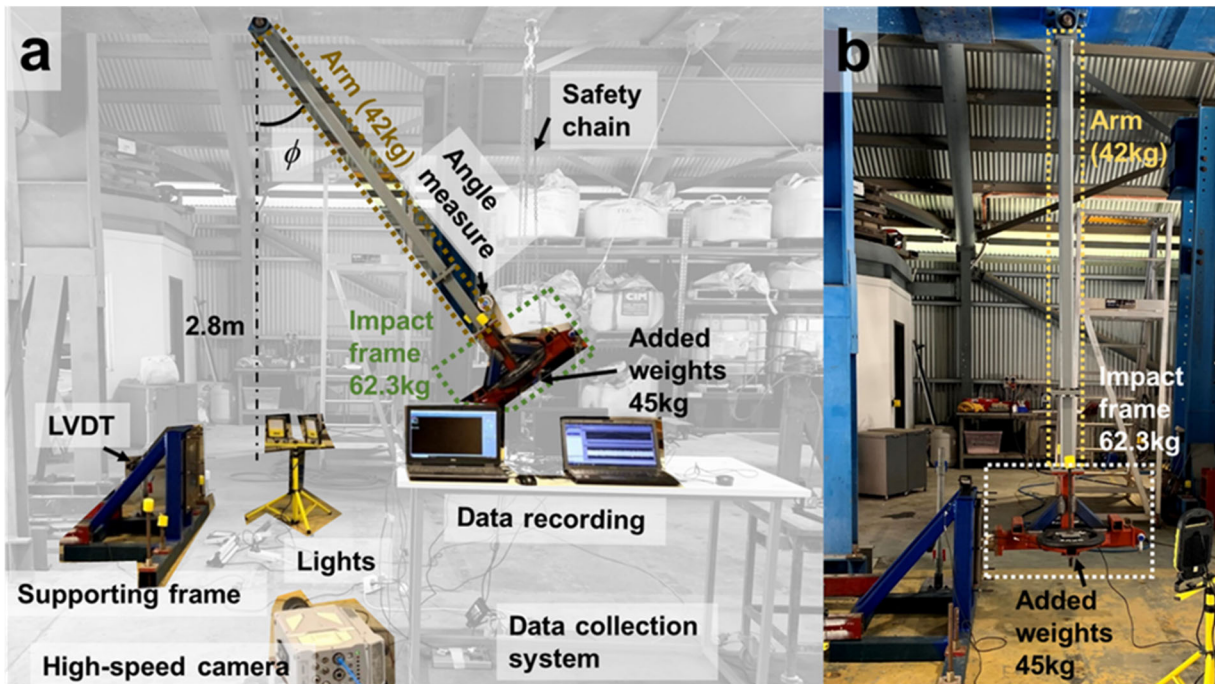


151

152 Figure 5. (a) True stress-strain curves of Aluminium 5052 H32 plate (front and rear plates)  
153 and Aluminium 1060 sheet (core); (b) Digital image correlation for local strain measurements  
154 of 5052 H32 specimen

155 **3 Pendulum impact testing**

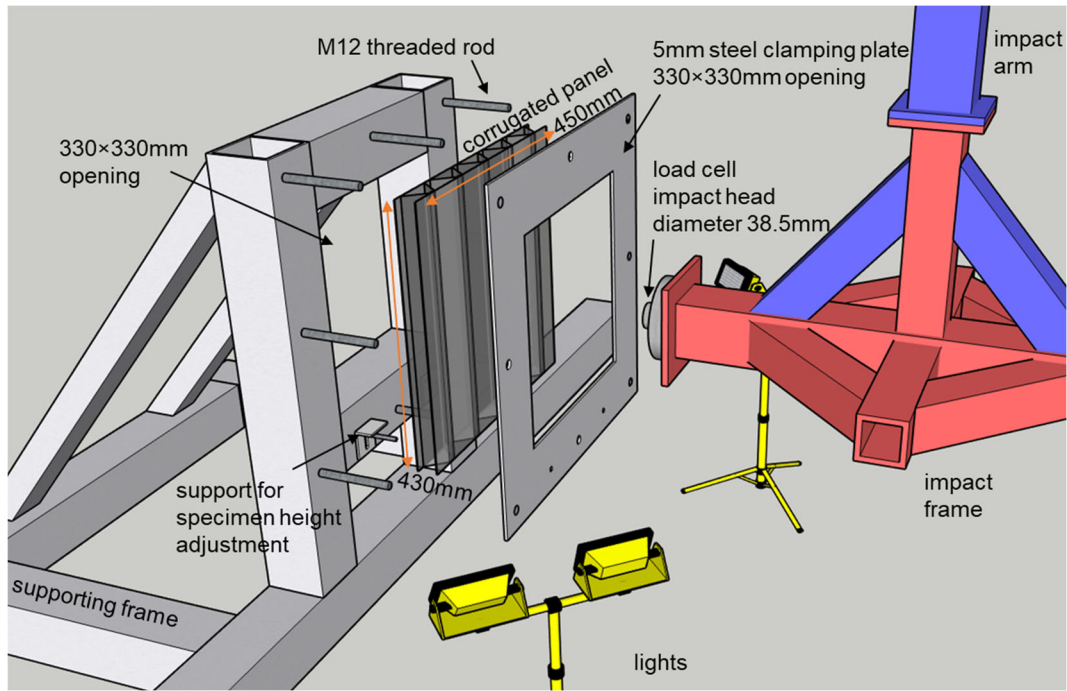
156 3.1 Experimental setup



157

158 Figure 6. (a) Pendulum impact testing setup; (b) Pendulum at resting position

159 The pendulum impact testing setup is shown in Figure 6. The pendulum consists of 2 sections,  
160 i.e. an arm with a mass of 42 kg and a 62.3 kg impact frame where extra weights can be added  
161 on. It has a total length of 2.8 m, measured from the top end to the impacting centre. The  
162 pendulum arm is made of square hollow section steel and its mass is distributed equally along  
163 the arm. The sandwich panels were placed vertically with 430 mm in length and 450 mm in  
164 width, then clamped between the supporting frame and a 5 mm steel plate using 8 M12 bolts,  
165 as shown in Figure 7. Two angles were used to support the panel to adjust the vertical position  
166 of the panel to ensure the impact at centre. Both front clamping steel plate and the supporting  
167 frame had square openings with the size of 330×330 mm. Two key parameters including impact  
168 force and displacement at the centre point of rear plate were recorded for each impact. Laser  
169 displacement transducer (LVDT) and load cell with a maximum range of 100 kN were used  
170 for measuring the displacement and impact force time histories. The impact head on the load  
171 cell had a diameter of 38.5 mm. High-speed videos were also captured for all tests.



172

173

Figure 7. Schematic diagram of the setup

174

The impact energy can be adjusted by controlling the impact mass and velocity, which is achieved by adjusting extra weights fixed on the impact frame and the release angle of the pendulum, respectively. The impacting velocity is the velocity of the pendulum at the moment of impact, when the pendulum is exactly vertical. By equalling the potential energy of the raised pendulum and kinetic energy at impact, the impacting velocity,  $v$ , can be calculated as

178

$$v = \sqrt{2gL_{arm}(1 - \cos\phi)} \quad (6)$$

179

where  $g$  is the gravity,  $L_{arm}$  is the length of the pendulum arm and  $\phi$  is the release angle of the pendulum. It should be noted that the friction and air drag forces are neglected.

180

181

To calculate the impact energy of each impacting scenario, the equivalent mass of the pendulum arm needs to be calculated. As the pendulum arm is not travelling at the same tangential velocity along the arm length, the velocity of pendulum arm at the bottom end is equal to impacting velocity,  $v$ , the velocity at the top end of the arm is zero and it is linearly

184

185

distributed along the arm. Therefore, the average velocity of the arm is  $\frac{v}{2}$ , and the equivalent

186 mass of the pendulum is converted using equation (7) and (8). For this conversion, the impact  
187 frame including the added weights is treated as a concentrated mass and the mass of pendulum  
188 arm (42 kg) is assumed to be equally distributed along its length.

$$\frac{1}{2}m_{arm}\left(\frac{v}{2}\right)^2 + \frac{1}{2}m_{frame}v^2 = \frac{1}{2}m_{eqv}v^2 \quad (7)$$

$$m_{eqv} = m_{frame} + \frac{m_{arm}}{4} \quad (8)$$

189  $m_{arm}$  is the mass of pendulum arm (42 kg),  $m_{frame}$  is the mass inside the green dashed box in  
190 Figure 6, which includes the mass of impact frame and any weight attached onto the impact  
191 frame. Using equation (8), the pendulum impact can be converted into direct impact with the  
192 equivalent mass of  $m_{eqv}$  and the impacting velocity of  $v$ .

193 Both pendulum impact and drop-weight impact tests as typical impact testing methods can be  
194 employed to investigate crushing behaviours of the panel. Single impact is ideal to compare  
195 and quantify the impact performance of panels. Multiple impacts are likely in the drop weight  
196 impact tests while the current pendulum impact test system can avoid multiple impacts in the  
197 test, which makes it more suitable for this study. Moreover, pendulum impact tests make it  
198 easier to monitor the deformation, especially the back face deformation of the tested specimens,  
199 as illustrated in this study.

### 200 3.2 Impacting scenarios

201 The overall test program is listed in Table 2. Each test is notated by specimen type, added  
202 weight on the pendulum, and impacting velocity. The letter 'B' for test 9 to 11 represents the  
203 back face (flipped panel) impact scenarios. In this study, two impacting masses were used, the  
204 pendulum with no added weight and with 45 kg extra weights (including 40 kg weight and 5  
205 kg of fixtures), where the overall mass for two cases equal to 104.3 kg and 149.3 kg

206 (104.3+45kg), respectively. The equivalent masses for these two scenarios were 73 kg and 118  
 207 kg, calculated using equation (8). The impact velocity of 3 m/s was selected as the reference  
 208 case based on preliminary numerical simulations. The corresponded release angle was then  
 209 determined as 33°. For the scenarios with 45kg of added weights, the impact speed was  
 210 calculated to be 2.36 m/s so that the same impact energy as the reference case (i.e. bare  
 211 pendulum, 3 m/s) of 328 J can be maintained in this study. The release angle of pendulum for  
 212 the impacting scenario with extra weight was then calculated to be 26°. Furthermore, back face  
 213 impacting tests for three corrugated panels were carried out in test 9 – 11 as given in Table 2.  
 214 Since the front and back sides of the corrugated cores are not symmetric, the impact response  
 215 for each configuration of panel could be different between the frontal and back impact.

216 Table 2. Pendulum impact test program

Test no.	Notation	Specimen	added weight	Impact velocity $v$	Release angle $\phi$	Equivalent impact mass $m_{eqv}$	Impact energy $\frac{1}{2}m_{eqv}v^2$
1	FL-73-3	Laminated flat plate	0 kg	3 m/s	33°	73 kg	328 J
2	CC-73-3	Conventional corrugated	0 kg	3 m/s	33°	73 kg	328 J
3	KC1-73-3	Kirigami corrugated 1	0 kg	3 m/s	33°	73 kg	328 J
4	KC2-73-3	Kirigami corrugated 2	0 kg	3 m/s	33°	73 kg	328 J
5	CC-118-2.36	Conventional corrugated	45 kg	2.36 m/s	26°	118 kg	328 J
6	KC1-118-2.36	Kirigami corrugated 1	45 kg	2.36 m/s	26°	118 kg	328 J

7	CC-73- 2.36	Conventional corrugated	0 kg	2.36 m/s	26°	73 kg	203 J
8	KC1-73- 2.36	Kirigami corrugated 1	0 kg	2.36 m/s	26°	73 kg	203 J
9	CC-B-73- 3	Conventional corrugated (back)	0 kg	3 m/s	33°	73 kg	328 J
10	KC1-B- 73-3	Kirigami corrugated 1 (back)	0 kg	3 m/s	33°	73 kg	328 J
11	KC2-B- 73-3	Kirigami corrugated 2 (back)	0 kg	3 m/s	33°	73 kg	328 J

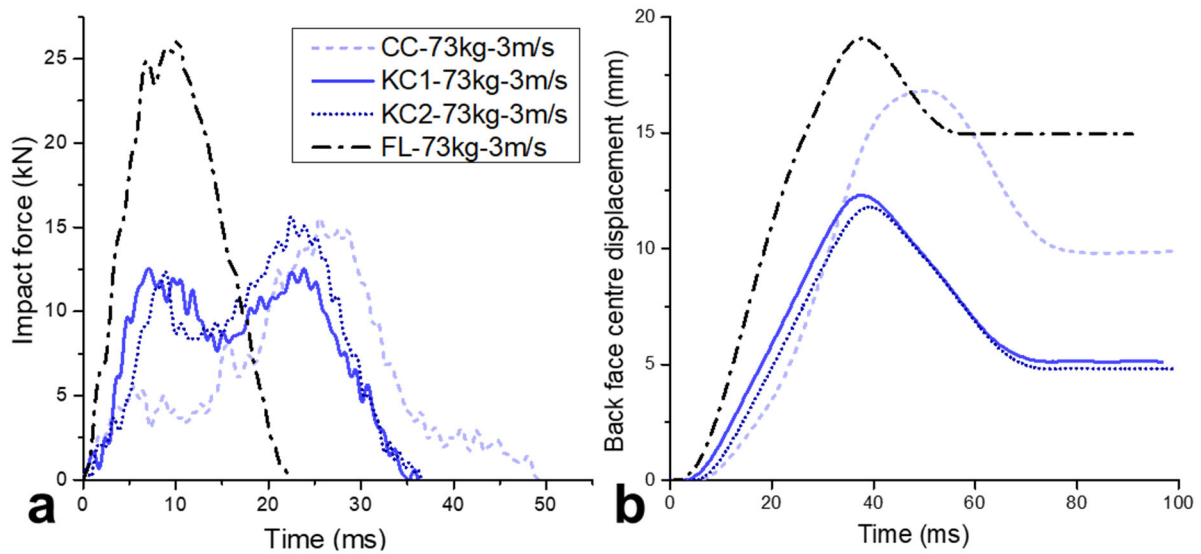
## 217 4 Results and discussions

### 218 4.1 Comparison among FL, CC, KC1 and KC2

219 Four configurations of panel specimens, including laminated flat plate (FL), conventional  
220 corrugated (CC), Kirigami corrugated 1 (KC1) and Kirigami corrugated 2 (KC2), were tested  
221 under the same loading condition. The scenario of the bare pendulum with equivalent mass of  
222 73 kg at 33° of impact angle is used as the reference for comparison and discussion of the  
223 performances of sandwich panels with corrugated core. The impact force time histories and  
224 rear face centre displacement time histories are shown in Figure 8, with key values listed in  
225 Table 3.

226 The laminated flat plate experienced the highest impact force and the largest centre  
227 displacement of the rear face. With regards to the rear plate deformation, the conventional  
228 corrugated plate CC outperformed the laminated plate with a 34% reduction in residual  
229 displacement at the centre of rear plate. Two Kirigami modified corrugated panel further

230 reduced the residual rear face displacement to around 5 mm, where KC2 configuration showed  
 231 slightly lower displacement than KC1. The duration of the impact obtained from the impact  
 232 force time histories varied, where CC panel had the longest impact duration followed by  
 233 KC1&2 panels and FL had the shortest impact duration. However, the impacting impulse  
 234 estimated by the area under the force time histories seems similar among the four tests.



235  
 236 Figure 8. (a) Impact force time histories; (b) rear plate centre displacement time histories; of  
 237 the laminated flat plate (FL), conventional corrugated (CC), Kirigami corrugated 1&2 (KC1 &  
 238 KC2) panels under 73 kg (bare pendulum), 3 m/s impact

239 Table 3. Peak and residual displacement, peak impact force of four panels under 73 kg impact  
 240 with an impacting velocity of 3 m/s

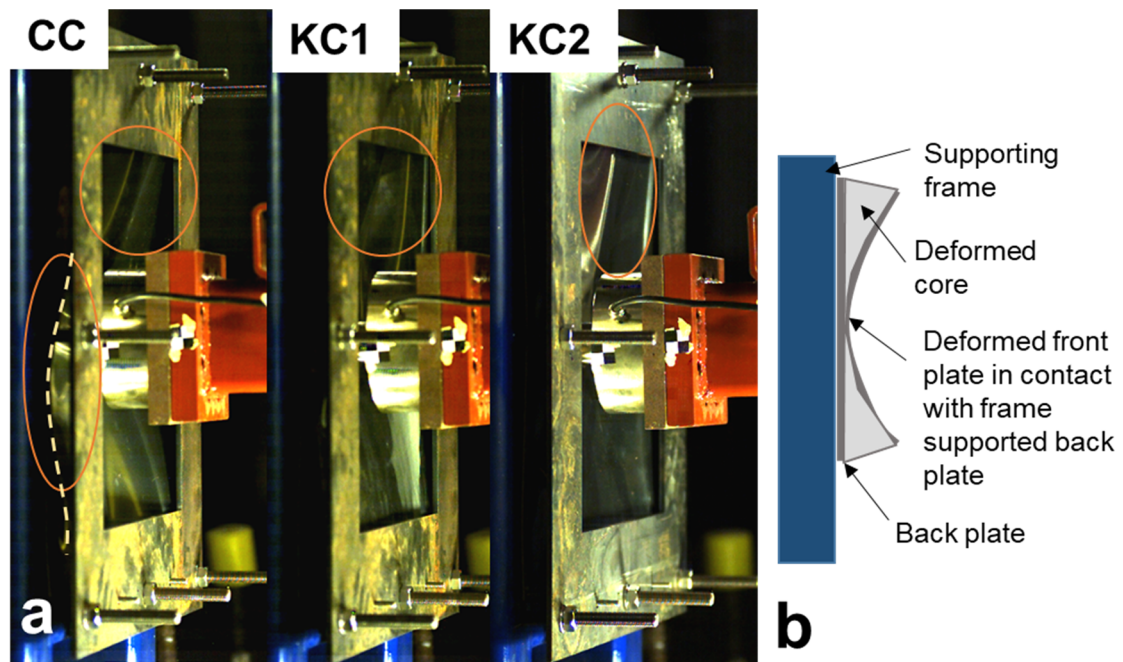
	Rear face centre displacement		Peak impact force
	Peak (mm)	Residual (mm)	(kN)
<b>FL</b>	19.1	14.9	26.3
<b>CC</b>	16.8	9.8	15.6
<b>KC1</b>	12.3	5.1	12.5
<b>KC2</b>	11.8	4.8	15.6

241 As shown in Figure 8 (a), the initial slopes of the impact forces are different among the panels,  
 242 depending on the local stiffness of the impacting location. The laminated plate shows a high

243 stiffness at the initial stage as the laminated plate FL does not have a soft core. The initial  
244 slopes fluctuate at first several milliseconds. KC1 panel seems to have a steeper slope in impact  
245 force from around 4 to 7ms than KC2 panel, as the impacting location is directly on top of a  
246 cell of KC1 and in-between two unit cells of KC2 panel, which leads to different contact  
247 stiffness at the initial stage of the impact. Furthermore, two peaks can be observed for three  
248 sandwich panels, CC, KC1 and KC2. The CC panel reaches its first peak in impact force earlier  
249 than other two corrugated panels, and its first peak is relatively low at around 4 kN. At the early  
250 stage of the impact up to 10 ms after contact, deformation on the rear plates of these three  
251 sandwiched panels are still minimal. Therefore, the peak in impact force at this stage mostly  
252 corresponds to the strength of the core near the impact area as well as the flexural stiffness of  
253 the front plate. Since the face plates on all panels are identical, a soft core, such as conventional  
254 corrugated core, can deform much easier than Kirigami corrugated core, resulting in a low peak  
255 at the early stage of impact. After this early stage of impact, the core and both face plates  
256 continue to deform until the densification of the core is reached and the deformed front plate  
257 is in partial contact with the rear plate, which leads to the second peak of the impact force.

258 As shown in Figure 8 (b), back plate starts to deform shortly after the impact. The back face  
259 deflection of laminated flat plate starts to increase at about 2 ms and it takes 6 ms for back face  
260 of sandwich panels to start deforming, due to the crushing of the core. Deformations of three  
261 sandwich panels, CC, KC1& KC2 at 25 ms after initial impact as shown in Figure 9 correspond  
262 to the second peak in impact force as shown in Figure 8(a). For both Kirigami corrugated panels,  
263 the front plate deformation concentrates near the top and centre of the panels, while the front  
264 plate is also severely deformed on the left side of the conventional corrugated sandwich panel.  
265 The severely deformed front plate indicates the localized densification of the core. As the outer  
266 edges are supported by the steel frame, the severely deformed front plate located around the  
267 outer edges. As illustrated in Figure 9 (b), severe deformation of the front plate along left side

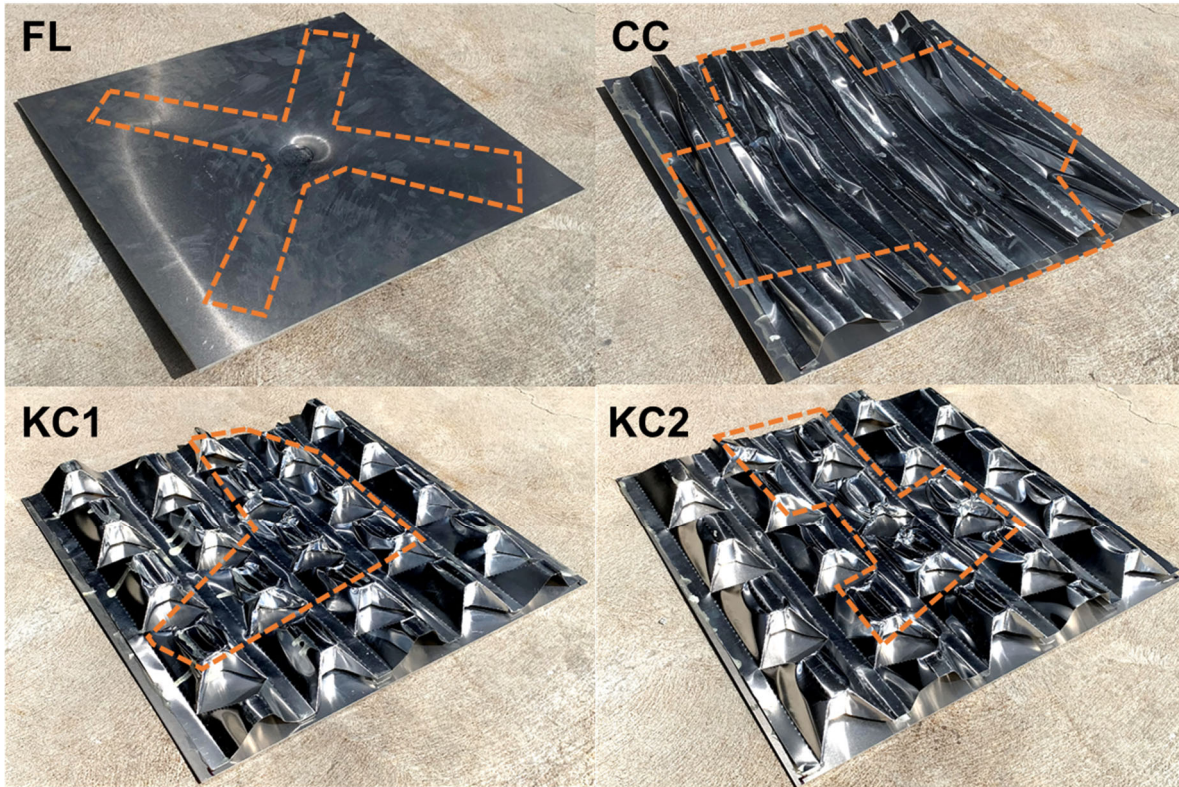
268 result in a sharp rise and a second peak in impact force. The impactor also starts to rebound  
269 after reaching the second peak, and the impact force decreases accordingly.



270

271 Figure 9. (a) High speed image of three sandwich panels at 25 ms of impact; (b) illustration  
272 of severely deformed front plate near the outer edges

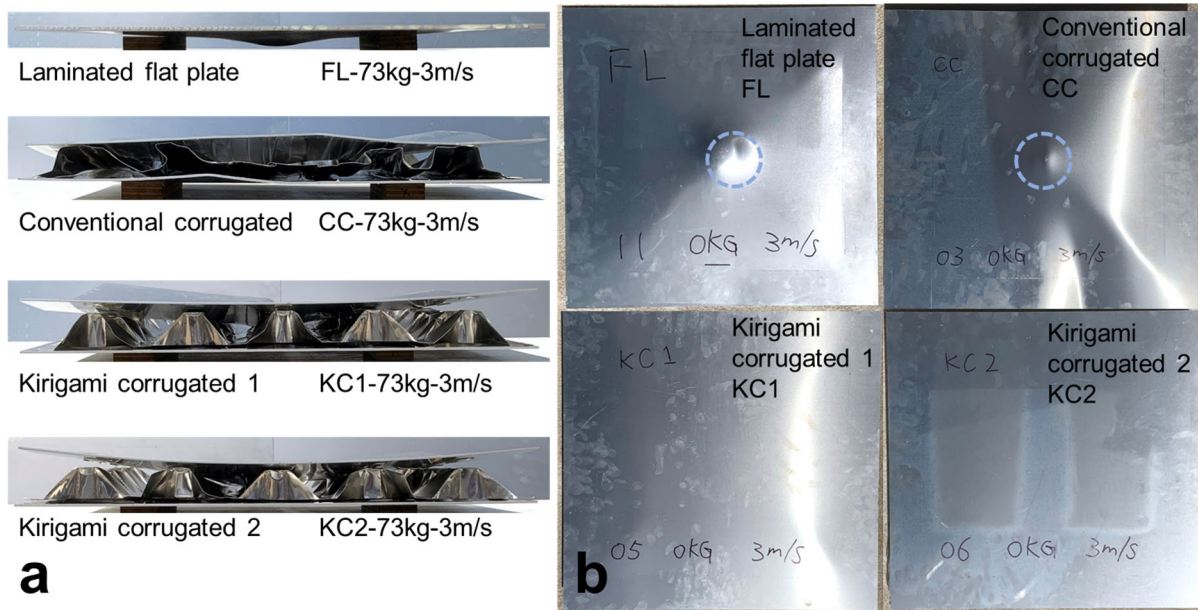
273 Furthermore, the difference in core strength leads to different loading duration as well as the  
274 maximum and residual rear face centre displacement. It should be noted that most of the panels  
275 debonded between the core and face plates after the impact, especially for the panels underwent  
276 large deformation, which was caused by the weak bonding strength between metal surfaces.  
277 Under the same impact scenario, the damage area of conventional corrugated core was much  
278 larger than that of Kirigami corrugated panels. As shown in Figure 10, the conventional  
279 corrugated core experienced severe damage with most of the core fully crushed. For Kirigami  
280 corrugated cores, the damage can only be observed near the impact location and a small portion  
281 propagated to one or two edges, which were caused by the bending deformation of the front  
282 plate. The laminated plate showed typical bending deformation of a clamped plate with highly  
283 concentrated damage at the impact location and the bending along two diagonals.



284

285 Figure 10. Front plate deformation of FL and core deformation of the three sandwiched  
286 panels with damaged areas marked out

287 The side view and rear face deformation are shown in Figure 11. Among the three corrugated  
288 panels, energy absorption capacity of the conventional corrugated core is insufficient to fully  
289 absorb the impact energy, even though the majority of the core was fully crushed. Therefore,  
290 both face plates of CC panel underwent larger deformation as compared to the Kirigami  
291 corrugated panels, which resulted in longer impact duration as well. Similar deformation mode  
292 with localized centre damage and deformation along diagonals were also observed for a thinner  
293 CC panels under foam projectile impact [30]. As shown in Figure 11 (b), both KC1 and KC2  
294 panel show minimal deformation on rear plate, with almost no noticeable localized damage at  
295 the impact location. Besides the local buckling damage, the overall deformation of rear plate  
296 might be also contributed by the secondary membrane effect of panel, which is not discussed  
297 in this study. Numerical simulation is deemed necessary in the future to determine the  
298 contribution from the secondary membrane effect.

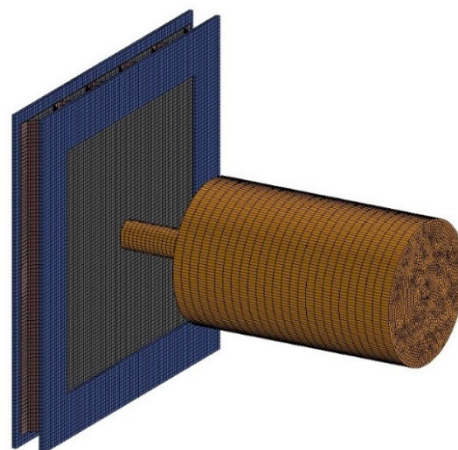


299

300 Figure 11. (a) Side view of four panels after impact; (b) rear plate deformation of four panels  
301 after impact

#### 302 4.2 Energy absorption obtained from numerical simulation

303 Due to the measurement limitation in the tests, the displacement histories of the impactor were  
304 not acquired, and the energy absorption of the corrugated panels were estimated using the  
305 validated finite element models. For the laminated plate, compression deformation at the centre  
306 of the plate is minimal, therefore the back displacement is almost identical as the front plate,  
307 and the measured data can be used to calculate the work done by the applied load and hence  
308 the energy absorption of the laminated plate.

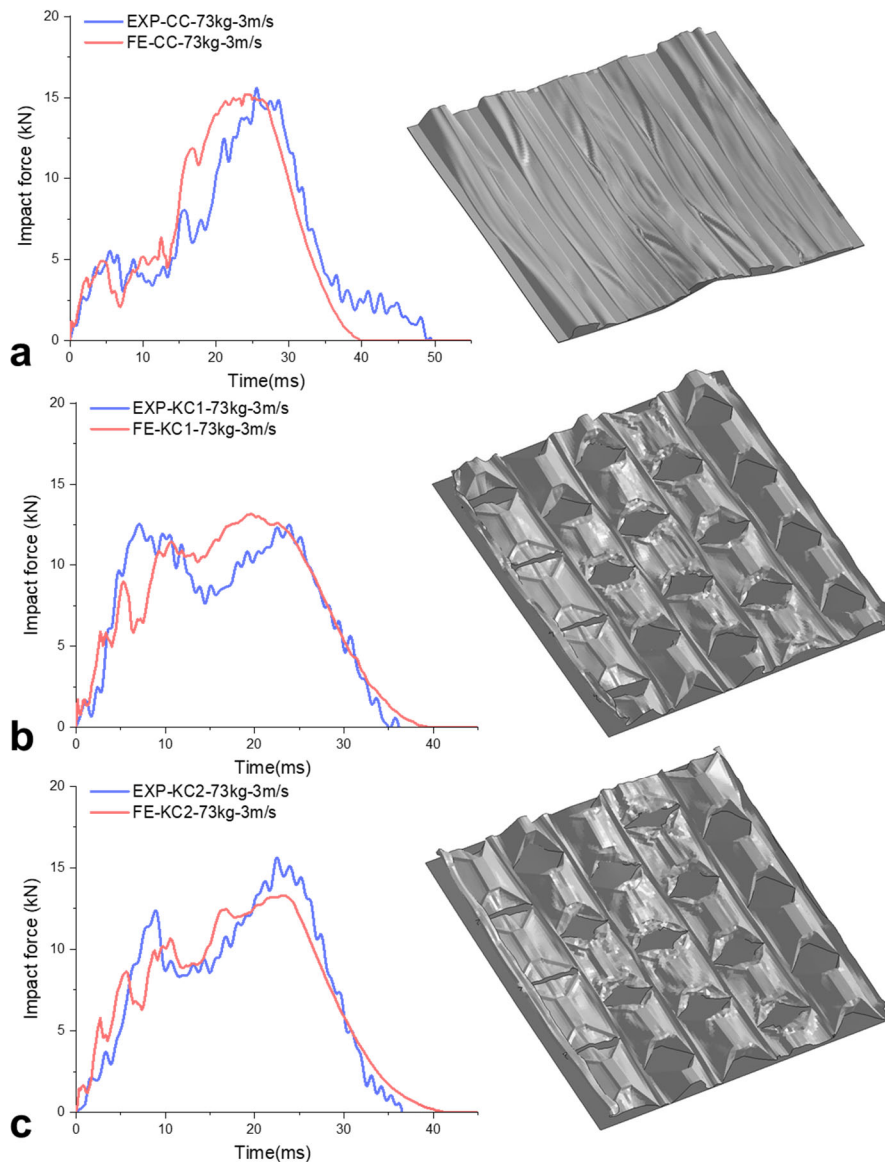


309

310 Figure 12. Numerical model of the corrugated panel under 73 kg, 3 m/s impact

311 To evaluate the energy absorption performances of the proposed Kirigami modified corrugated  
312 structure, numerical simulation of these three sandwich panels (KC1, KC2 and CC under 73kg  
313 impact at 3 m/s) were carried out by using finite element software LS-DYNA. The impactor in  
314 the numerical model was simplified as a mass of 73 kg with an initial speed of 3 m/s as shown  
315 in Figure 12. Piecewise linear plastic material model was used for the sandwich panels and  
316 their material parameters were taken from the measured data in section 2.2. The panels were  
317 constructed using Belytschko–Tsay type shell element, clamping plates and impactor were  
318 modelled using rigid solid element. Other keywords used in LS-DYNA were kept the same as  
319 in the previous study [29].

320 The impact force-time histories from FE (finite element) simulations and tests, as well as the  
321 deformation mode from FE results are shown in Figure 13. As shown, the FE model well  
322 predicts the force-time histories in the test. Two peaks in impact force are shown for all three  
323 cases. As discussed in 4.1, the first peak in impact force corresponds to the crushing strength  
324 of the core at the impacting area and the flexural stiffness of the front plate, therefore the CC  
325 panel has a lower first peak in impact force than KC1 and KC2 due to its lower compressive  
326 strength of the core. The second peak in impact force caused by the partial contact between the  
327 front and supported back plate due to core densification is also captured by FE simulations.  
328 The deformations of these three panels agree with the test results, where the centre units and  
329 some of the units near the edge are crushed for KC panels. Some slight discrepancies between  
330 FE and test results in impact force-time histories and deformation mode may be caused by the  
331 perfect geometry of the panels and bonding properties of epoxy in the numerical model. Overall,  
332 the FE results are in good agreement with the test data, and the FE model is acceptable for  
333 evaluating the energy absorption of the three sandwich panels.



334

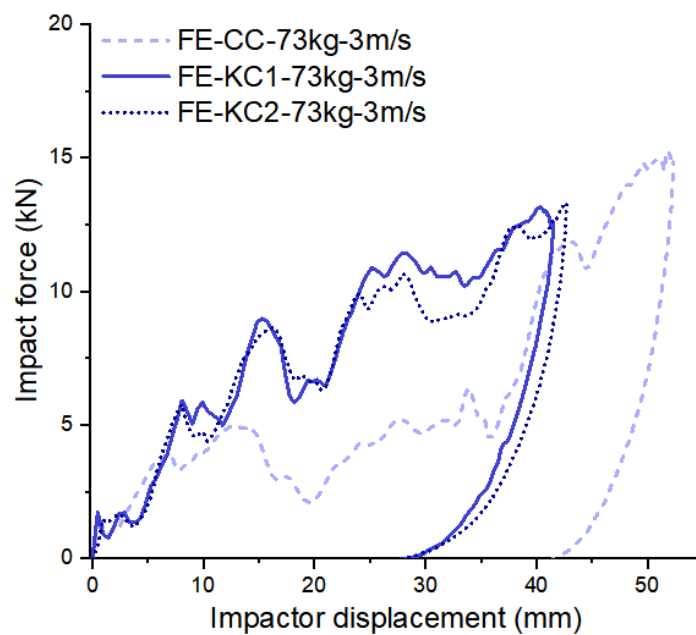
335 Figure 13. Impact force-time histories and deformation mode comparisons for (a) CC; (b)  
 336 KC1; (c) KC2 sandwich panels under 73 kg, 3m/s impact

337 The curves of impact force and impactor displacement are shown in Figure 14. Energy  
 338 absorption of three sandwiched panels are estimated by integrating the respective impact force-  
 339 impactor displacement curve and the results are listed in Table 4. The energy absorption of the  
 340 laminated plate (FL) was calculated from the testing data. This is because the laminated plate  
 341 has no crushable core and its compressive deformation along the thickness can be neglected,  
 342 thus the measured back plate displacement is the same as that of the front plate where impact  
 343 force is applied. Three sandwich panels show significant improvement in energy absorption  
 344 comparing to the laminated plate (FL), while the both KC panels have similar energy

345 absorption to the CC panel. Despite the similar absorbed energy by the three panels (CC, KC1  
 346 and KC2), the core of the both KC panels absorbed significantly higher amount of energy than  
 347 that of the CC panel, since the back plate of the CC panel experienced much severe plastic  
 348 deformation than that of the both KC panels as demonstrated in Figure 11. Figure 14 suggests  
 349 the similar conclusions. Compared to the KC panels, large area is enclosed in the impact force-  
 350 displacement curve towards the later stage of the loading for the CC panel and the sudden rise  
 351 in impact force at around 35 mm of displacement indicates the full compaction of the core for  
 352 the CC panel. Overall, the Kirigami modified corrugated panels show significant improvement  
 353 in energy absorption capacities of the core, and the reduction in back plate deformation as  
 354 compared to the conventional corrugate panel, indicating an enhanced impact resistance  
 355 capacity and energy absorbing performance.

356 Table 4. Estimated energy absorption of the four panels under 73 kg, 3 m/s impact

Items	FL (test)	CC (FE)	KC1 (FE)	KC2 (FE)
Energy absorption (J)	194	280	282	280

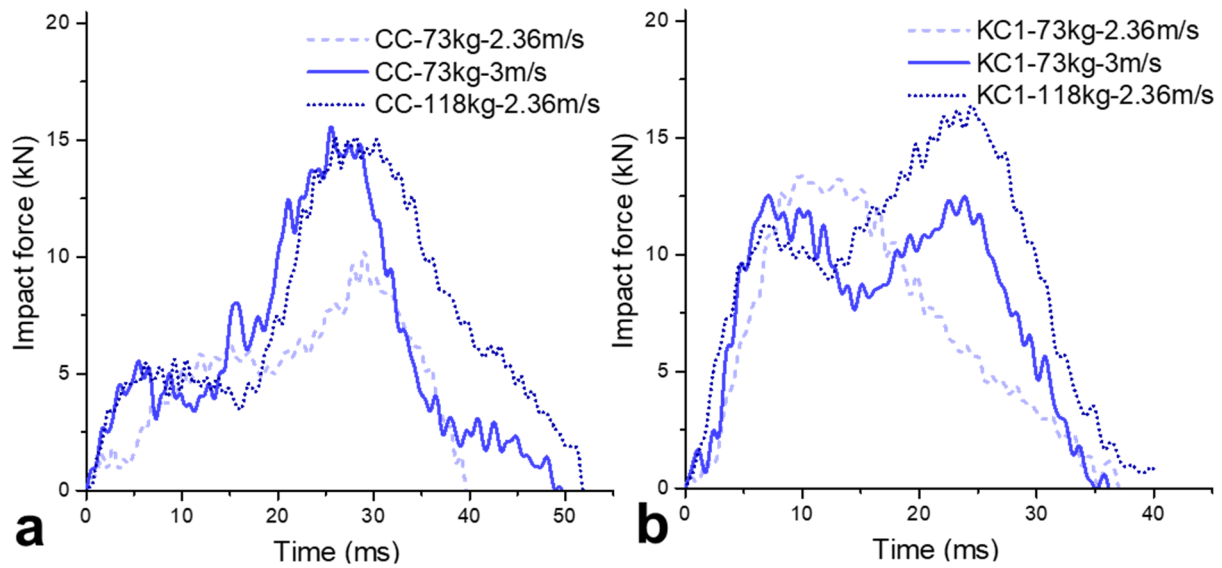


357

358 Figure 14. Impact force versus impactor displacements of the three sandwiched panels under  
 359 73kg, 3m/s impact

### 360 4.3 Effect of impact mass and velocity

361 Different impact scenarios were considered to investigate and compare the impact resistance  
362 of conventional corrugated and Kirigami corrugated panels. Two impact masses, one with bare  
363 pendulum and the other with 45 kg of added weight were included, where the equivalent mass  
364 for the two cases are 73kg and 118 kg respectively. Two impact velocities of 2.36 and 3m/s  
365 were included as well. It should be noted that the case of 118kg-2.36 m/s impact was selected  
366 to match the impact energy of the 73kg-3m/s impact case. However, the impacting impulse is  
367 not equal among the three scenarios. The impact force and back centre displacement time  
368 histories are shown in Figure 12 and Figure 13. The key parameters are listed in Table 4. It can  
369 be observed that the KC1 panel outperformed the CC panel with a reduced peak and residual  
370 displacement on rear plate under all impact scenarios. The residual rear face centre  
371 displacement of KC1 panel was reduced up to 48%, compared to CC panel. However, different  
372 variation in general trend of impact force time history for the two panels with the changes in  
373 impact scenarios was observed. As shown, increasing the impact velocity from 2.36 m/s to  
374 3.0m/s, the impact force acting on CC panel increases substantially; the peak impact force of  
375 the two cases with the same kinetic impacting energy, namely 118 kg-2.36 m/s and 73 kg-3.0  
376 m/s, induces almost the same peak impact force, but the duration of the case with 118 kg-2.36  
377 m/s is longer. The changes in the impact force profile on KC1 panel by varying the impacting  
378 velocity and mass are different from those on CC panel. As shown, at the smaller kinetic impact  
379 energy with 73 kg-2.36 m/s, there is only one impact pulse on KC1 panel, increasing the kinetic  
380 impact energy by either increasing the impact mass or velocity, two impact pulses are observed,  
381 and impact with 118kg-2.36 m/s generates higher peak impact force and longer impact duration.

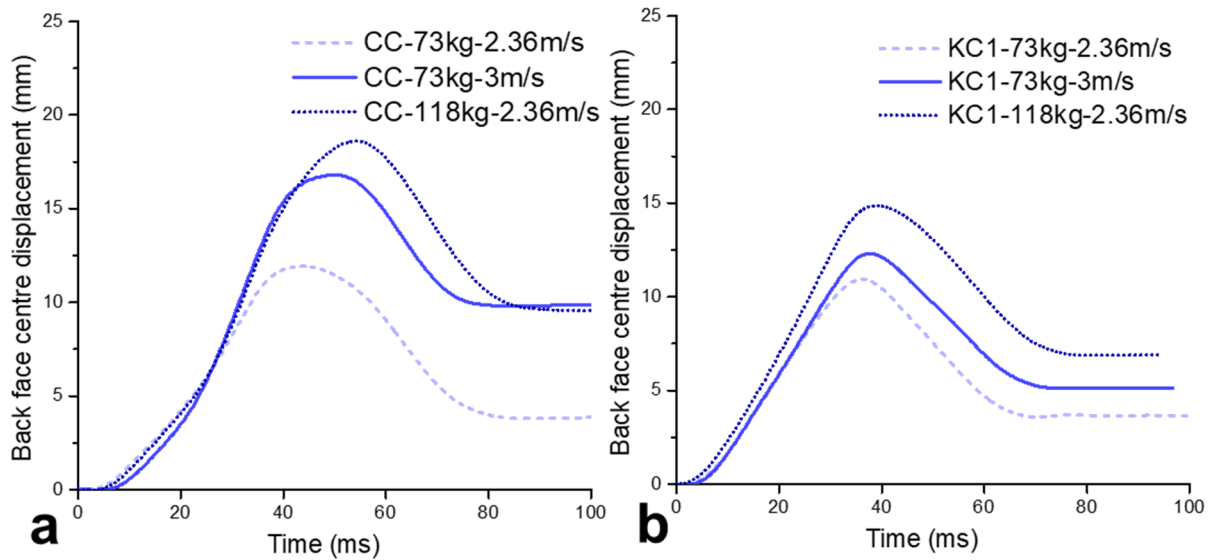


382

383

384

Figure 15. Impact force time histories of (a) conventional corrugated (CC) panels; (b) Kirigami corrugated 1 (KC1) panels under different impact scenarios



385

386

387

Figure 16. Rear face centre displacement time histories of (a) conventional corrugated (CC) panels; (b) Kirigami corrugated 1 (KC1) panels under different impact scenarios

388

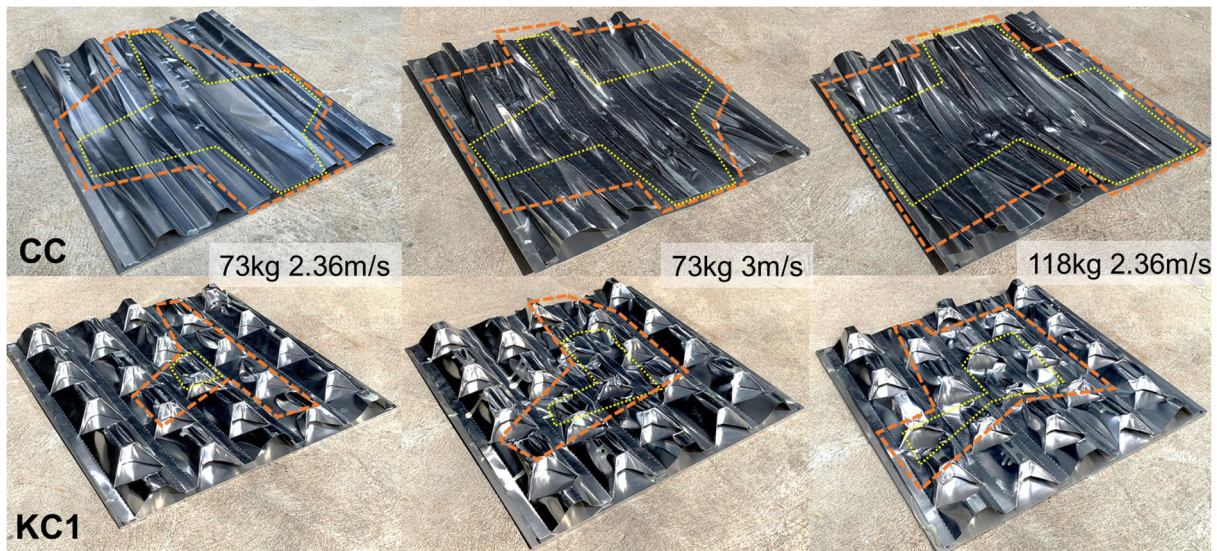
389

Table 5. Peak and residual displacement, peak impact force for CC and KC1 panels under different impact scenarios

Impact scenarios	Core type	Rear face centre displacement		Peak impact force (kN)
		Peak (mm)	Residual (mm)	
73kg-2.36m/s	CC	11.9	3.9	10.2
	KC1	10.9	3.7	13.4

<b>73kg-3m/s</b>	CC	16.8	9.8	15.6
	KC1	12.3	5.1	12.5
<b>118kg-3m/s</b>	CC	18.6	9.6	15.2
	KC1	14.9	6.9	16.4

390 Despite the difference in impact force profiles, the first peak of impact force is of similar value  
391 for each panel. As previously discussed, the first peak of impact force depends primarily on  
392 the contact between the impactor and the front plate, as well as the core strength and the flexural  
393 stiffness of the front plate, besides the impact mass and velocity. Therefore, the first peak of  
394 impact force remains at a similar level because of the same impact scenario and the same front  
395 plate, as well as the similar deformation on the front plate and the core. However, the second  
396 peak in impact force profile developed differently for the two panels under different impact  
397 scenarios. For the case of 73kg-2.36m/s, the second peak in impact force can be observed for  
398 CC panel but not for KC1 panel. A large portion of the conventional corrugated core of CC  
399 panel was fully crushed and the front plate underwent large deformation, which led to the  
400 partial contact with the rear plate to induce the second peak of impact force. For KC1 panel,  
401 only a small portion of core was deformed and the densification of the core was not reached as  
402 shown in Figure 14 and Figure 15 (a), thus a second peak was not observed.

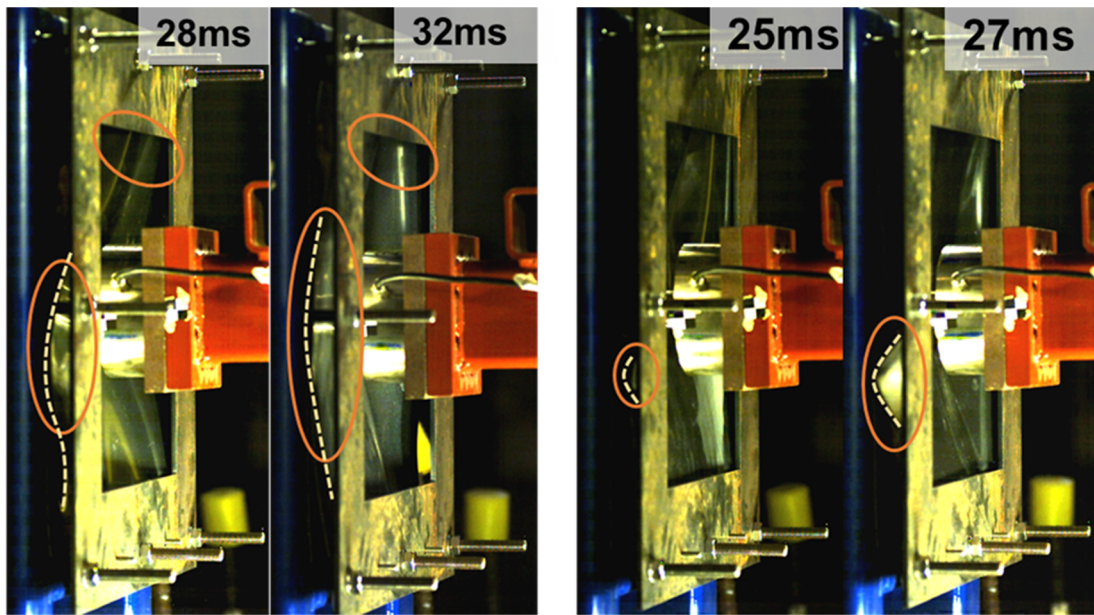


403

404 Figure 17. Core deformation of CC and KC1 panels under different impact scenarios with  
 405 partially and fully crushed areas marked in orange and yellow, respectively

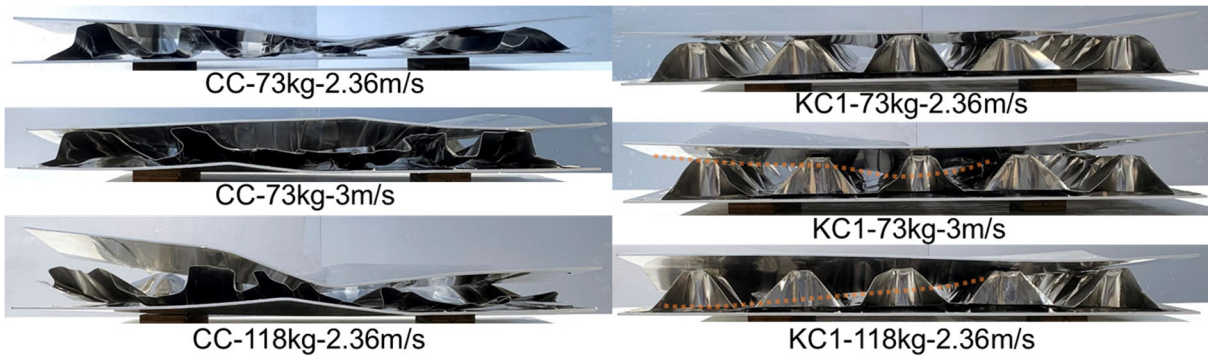
406 For CC panels, the second peak of impact force remained in similar level when impact scenario  
 407 changed from 73kg-3m/s to 118kg-2.36m/s, however the second peak in impact force increased  
 408 for KC1 panels. As marked out in Figure 14 and Figure 15, the damaged area of CC panels  
 409 only slightly increased when impact scenario changed from 73kg-3m/s to 118kg-2.36m/s, as a  
 410 majority of the core was damaged in both cases. As previously shown in Figure 9, the front  
 411 plate of CC-73kg-3m/s underwent severe deformation along the side and it partially contacted  
 412 the rear plate which was supported by a rigid frame, resulting in the spike in impact force.  
 413 Therefore, further increase of impacting impulse may not lead to an increase in the second peak  
 414 of impact force for CC panel. For KC1-73kg-3m/s, the deformation on the front plate was  
 415 moderate compared to CC panel, and the front plate was not in contact with the supported rear  
 416 plate (Figure 15). Therefore, its second peak of impact force is less than that of CC panel under  
 417 the same impact. However, changing the impact scenario led to an increase in impacting  
 418 impulse (from 73kg-3m/s to 118kg-2.36m/s) as shown in Figure 12 (b), although the impact  
 419 kinetic energy remained the same but the interaction between the impactor and the KC1 panel  
 420 changed, it resulted in the deformation of a larger portion of the front plate and core of KC1

421 panel, and hence the partial contact with the rear plate as marked out in Figure 16, which  
 422 induced the second peak of impact force as shown in Figure 12 (b).



423 CC-73kg-3m/s CC-118kg-2.36m/s KC1-73kg-3m/s KC1-118kg-2.36m/s

424 Figure 18. High speed image of CC and KC1 panel under 73kg-3m/s and 118kg-2.36m/s  
 425 impact at the moment of maximum deformation of the front plate



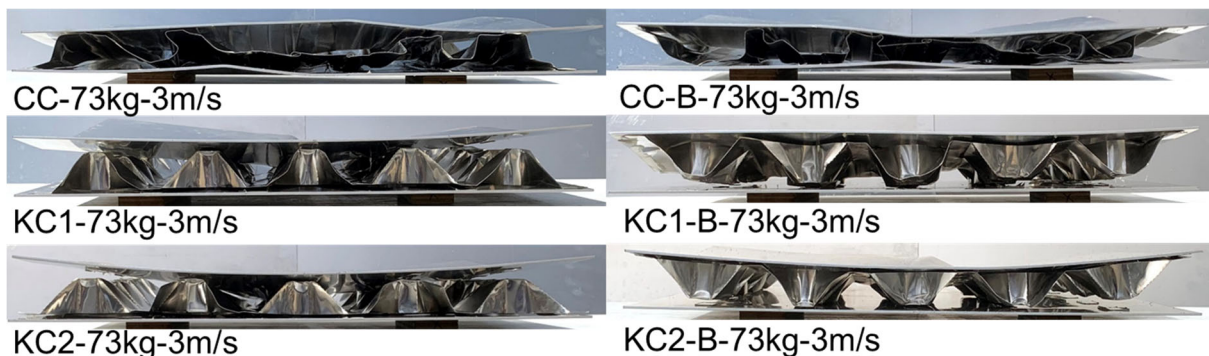
426 CC-73kg-2.36m/s KC1-73kg-2.36m/s  
 427 CC-73kg-3m/s KC1-73kg-3m/s  
 428 CC-118kg-2.36m/s KC1-118kg-2.36m/s  
 429 Figure 19. Side view of deformed panels under different impact scenarios, the top plate  
 428 deformation is marked out in dash lines for KC1 panels

429 For the same reason, two panels CC and KC1 showed different trends of the displacement time  
 430 histories at the centre of rear plate. The residual displacements at the centre of rear face were  
 431 similar for CC-73kg-3m/s and CC-118kg-2.36m/s, but it increased for KC1 panel when impact  
 432 load changed from 73kg-3m/s to 118kg-2.36m/s. For CC-73kg-3m/s, the front plate was in  
 433 partial contact with the rear plate, especially near the outer edges where rear plate was  
 434 supported by the frame. Therefore, as shown in Figure 16, the front plate of CC panel

435 underwent more deformation while the core had the similar damage when the impact scenario  
436 changed from 73kg-3m/s to 118kg-2.36m/s. The deformed front plate of CC-118kg-2.36m/s  
437 resulted in a larger contact with the outer edges of the supported rear plate. Differently, for  
438 KC1 panel, the deformation on front plate and core increased slightly when impact scenario  
439 was changed from 73kg-3m/s to 118kg-2.36m/s. Only a small portion of the front plate was in  
440 contact with the outer edge of rear plate for KC1-118kg-2.36m/s, as marked out in Figure 16.

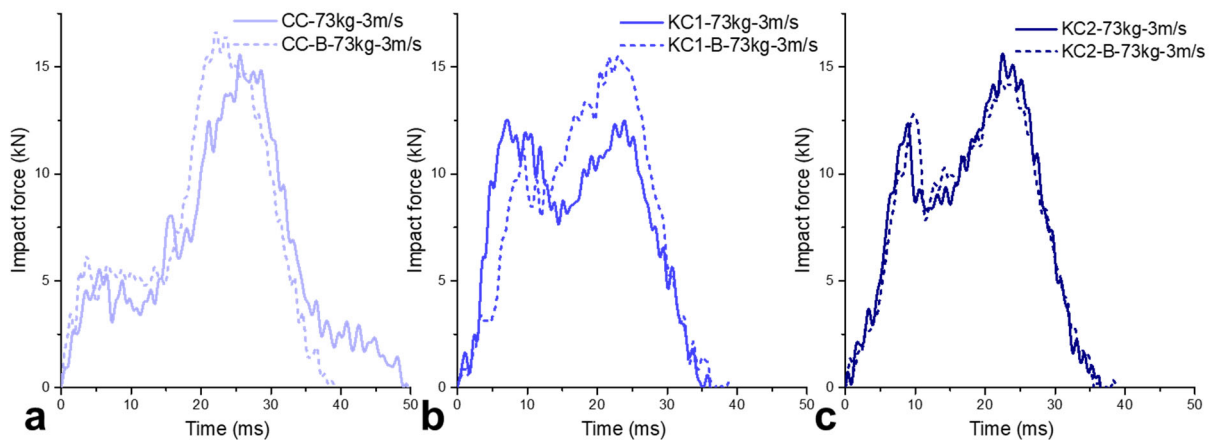
#### 441 4.4 Back panel impact

442 Since the cores are not symmetric between the front and back portion for all three sandwich  
443 panels, the back face impact scenario is considered in this section. Same impact loads as the  
444 reference tests (73kg-3m/s) were used where three panels including CC, KC1 and KC2 were  
445 flipped and impacted. The deformed panels for both impacting scenarios (frontal and back  
446 impact) are shown in Figure 17. It can be observed that debonding between the core and plates  
447 occurred on the concaved side of the corrugated core.



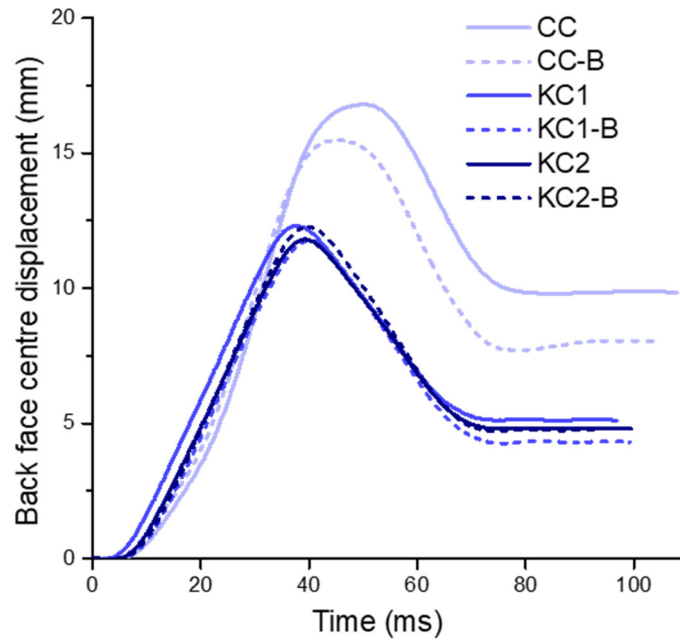
448  
449 Figure 20. Side view of deformed panels under 73kg-3m/s (L) frontal and (R) back impact  
450 The comparisons of impact force time histories among the panels subjected to the front and  
451 back impact are shown in Figure 18 and the rear face centre displacement time histories are  
452 shown in Figure 19. As shown, both Kirigami corrugated panels (KC1, KC2) show superior  
453 impact resistance as compared to the conventional corrugated panel (CC) under both the front  
454 and back impacts. The residual displacement at the centre of the rear face of KC panels reduced

455 around 40%, compared to CC panels. The KC2 panel showed almost identical impact force  
 456 and displacement time histories under both the front and back impacts. However, the induced  
 457 impact forces on CC and KC1 panels were slightly different when impacted on the front and  
 458 back face of the panels. For both the CC and KC1 panels, the impact force time histories show  
 459 an increased 2<sup>nd</sup> peak when the panels were impacted on the back face. The maximum impact  
 460 force increased by about 7% and 23% for CC and KC1 panels when they were impacted on the  
 461 back face. The maximum impact force reduced slightly for KC2 panel when impacted on the  
 462 back face. The residual displacements also decreased for CC and KC1 panels when impacted  
 463 on the back face. As listed in Table 5, the residual rear face centre displacement reduced nearly  
 464 2 mm for CC panel and 0.8 mm for KC1 panel when the panels were flipped and impacted. For  
 465 KC2 panel, however, both the peak and the residual displacements remained similar under both  
 466 impact scenarios.



467

468 Figure 21. Impact force time histories of front and back face impact for (a) CC; (b) KC1 and  
 469 (c) KC2 panels



470

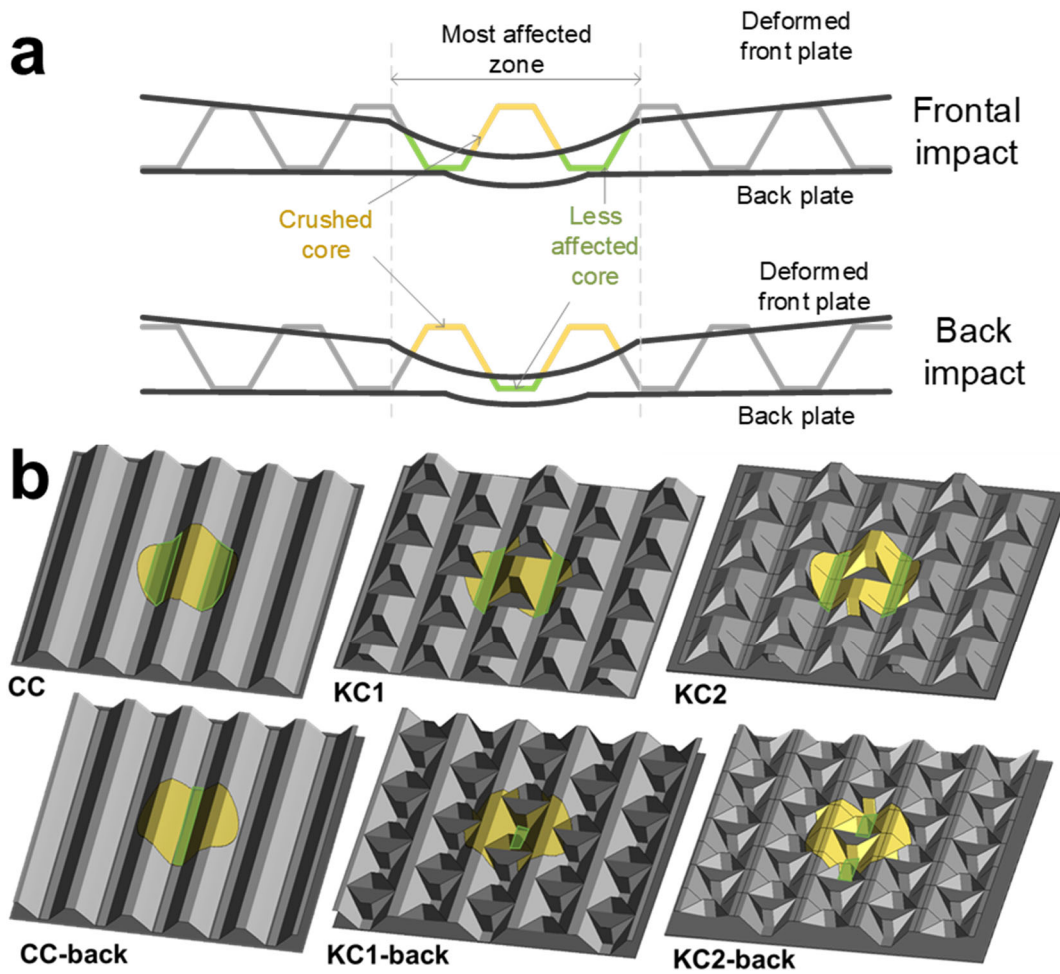
471 Figure 22. Rear face centre displacement time histories of CC, KC1 and KC2 panels under  
 472 the frontal and back impact of 73kg at 3m/s

473 Table 6. Peak and residual displacement, peak impact force on the three panels under frontal  
 474 and back impact

Core type	Rear face centre displacement		Peak impact force (kN)
	Peak (mm)	Residual (mm)	
<b>CC</b>	16.8	9.8	15.6
<b>CC-B</b>	15.5	8.0	16.7
<b>KC1</b>	12.3	5.1	12.5
<b>KC1-B</b>	11.8	4.3	15.5
<b>KC2</b>	11.8	4.8	15.6
<b>KC2-B</b>	12.3	4.8	14.4

475 The slightly improved impact resistance of CC and KC1 panels could be caused by the change  
 476 of core geometries when the panels were impacted on the back face. Due to the clamped  
 477 boundary, localized deformation and resistance of the core and face plate, the mostly deformed  
 478 area of the core is around its centre impacted area. Therefore, the change of core geometry in  
 479 the mostly deformed area caused by the flipping of the panel could lead to a slight change in

480 impact resistance. The impact resistance provided by the central area of the core can be  
481 different when the same panel is flipped, as the cores are not symmetric in the out-of-plane  
482 direction. A 2D illustration of the most deformed area of the corrugated panel is shown in  
483 Figure 20 (a), where the most deformed core is marked out in yellow and less deformed core  
484 is mark out in green. As both the KC panels are 3D structures, 3D illustration of the three panels  
485 under both impact scenarios is shown in Figure 20 (b) with similar mark out. For instance,  
486 under frontal impact the bottom section of the central area of CC, as marked out in green colour,  
487 contributed less as compared to the top portion of the central core. The green shaded area of  
488 the core was glued to the rear plate and underwent minimal deformation than top portion as  
489 rear plate deformed much less compared to the front plate. Thus, less energy per volume was  
490 absorbed by this section as compared to the rest of the central area of the core, such as the  
491 sidewalls and the top face which were bonded to the front plate. Once the CC panel was flipped,  
492 this section of core changed, the area which was bonded to rear plate reduced as shown in  
493 Figure 20, CC-back. Therefore, the impact resistance of CC panel slightly increased when the  
494 panel was flipped and impacted. Similarly, the KC1 panel shows a slightly reduction in the  
495 area that bonded to the rear plate in the central area when the panel was flipped and impacted.  
496 Different from CC panel, Kirigami corrugated core has a much higher crushing resistance due  
497 to the vertical fold-ins and the constraints provided to the adjacent side walls. The top face of  
498 each Kirigami corrugate unit cell contributed little to its crushing resistance. Therefore, the  
499 residual rear face displacement only reduced about 0.8 mm when the KC1 panel was flipped  
500 and impacted, where CC panels reduced about 2 mm. For the KC2 panel, the difference  
501 between the frontal and back impact scenarios is less, due to the core geometries as shown in  
502 Figure 20. Similar residual back centre displacement is observed for KC2 panels under frontal  
503 and back impacts.



504

505 Figure 23. (a) 2D illustration of centre area for the corrugated panel under frontal and  
 506 back impact; (b) Centre area (in yellow and green) of the core of each panel under both the frontal  
 507 and back impacts

## 508 5 Conclusion

509 In this study, impact response of a newly proposed sandwich panel with Kirigami modified  
 510 corrugated core was experimentally investigated with pendulum impact tests. The results were  
 511 compared with those of the conventional corrugated sandwich panel and laminated flat plate  
 512 subjected to the same impacts. Main conclusions can be drawn below.

513 1. The feasibility of the manufacturing process of the proposed Kirigami modification was  
 514 examined. Compared to the current modifications on the conventional corrugated core, the  
 515 proposed Kirigami modification shows minimal change to the manufacturing process of the  
 516 conventional corrugated core with multiple cells.

517 2. Under the same impact with the equivalent mass of 73 kg at 3 m/s, the conventional  
518 corrugated sandwich panel outperformed the laminated flat plate with a 34% reduction in the  
519 residual centre displacement of rear face. Kirigami modification further reduced the rear plate  
520 deformation of the corrugated sandwich panel by an additional 48%.

521 3. Different to the conventional corrugated panels where most of the core were crushed after  
522 the impact tests, the core of Kirigami corrugated panels only deformed around the impacting  
523 area with reduced deformations on the rear plate, demonstrating a higher crushing resistance  
524 and improved impact resistance of the Kirigami modified corrugated panels over the  
525 conventional corrugated sandwich panel, despite the reduction in longitudinal flexural stiffness  
526 of KC panels.

527 4. Different impact scenarios were also considered for conventional corrugated and Kirigami  
528 modified corrugated panels. It is found that the 1<sup>st</sup> peak impact force is associated with the core  
529 strength and a 2<sup>nd</sup> peak in impact force profile can be induced due to compaction of the core  
530 under higher impact loads. To examine the effect of impact locations, three corrugated  
531 sandwich panels were also impacted on the back face. It was found that impact resistance of  
532 CC and KC1 panels were slightly improved under back impact while KC2 panel showed almost  
533 identical impact responses under the frontal and back impact.

## 534 **Acknowledgement**

535 The authors acknowledge the support from the Australian Research Council via Discovery  
536 Early Career Researcher Award (DE160101116) to conduct this research work.

## 537 **References**

538 [1] M.A. Abteu, F. Boussu, P. Bruniaux, C. Loghin, I. Cristian, Ballistic impact mechanisms  
539 – A review on textiles and fibre-reinforced composites impact responses, *Composite Structures*,  
540 223 (2019) 110966.

- 541 [2] B. Castanie, C. Bouvet, M. Ginot, Review of composite sandwich structure in aeronautic  
542 applications, *Composites Part C: Open Access*, 1 (2020).
- 543 [3] A.G. Evans, J.W. Hutchinson, N.A. Fleck, M.F. Ashby, H.N.G. Wadley, The Topological  
544 Design of Multifunctional Cellular Metals, *Progress in Material Science*, 46 (2001) 309-327.
- 545 [4] H.N. Wadley, Multifunctional periodic cellular metals, *Philos Trans A Math Phys Eng Sci*,  
546 364 (2006) 31-68.
- 547 [5] Z. Li, W. Chen, H. Hao, Numerical study of sandwich panel with a new bi-directional Load-  
548 Self-Cancelling (LSC) core under blast loading, *Thin-Walled Structures*, 127 (2018) 90-101.
- 549 [6] K.P. Dharmasena, H.N.G. Wadley, Z. Xue, J.W. Hutchinson, Mechanical response of  
550 metallic honeycomb sandwich panel structures to high-intensity dynamic loading, *International*  
551 *Journal of Impact Engineering*, 35 (2008) 1063-1074.
- 552 [7] F. Côté, V.S. Deshpande, N.A. Fleck, A.G. Evans, The compressive and shear responses of  
553 corrugated and diamond lattice materials, *International Journal of Solids and Structures*, 43  
554 (2006) 6220-6242.
- 555 [8] M.R.M. Rejab, W.J. Cantwell, The mechanical behaviour of corrugated-core sandwich  
556 panels, *Composites Part B: Engineering*, 47 (2013) 267-277.
- 557 [9] D.Y. Seong, C.G. Jung, D.Y. Yang, K.J. Moon, D.G. Ahn, Quasi-isotropic bending  
558 responses of metallic sandwich plates with bi-directionally corrugated cores, *Materials &*  
559 *Design*, 31 (2010) 2804-2812.
- 560 [10] V. Rubino, V.S. Deshpande, N.A. Fleck, The dynamic response of clamped rectangular  
561 Y-frame and corrugated core sandwich plates, *European Journal of Mechanics - A/Solids*, 28  
562 (2009) 14-24.
- 563 [11] G.K. Schleyer, M.J. Lowak, M.A. Polcyn, G.S. Langdon, Experimental investigation of  
564 blast wall panels under shock pressure loading, *International Journal of Impact Engineering*,  
565 34 (2007) 1095-1118.
- 566 [12] X. Li, Z. Wang, F. Zhu, G. Wu, L. Zhao, Response of aluminium corrugated sandwich  
567 panels under air blast loadings: Experiment and numerical simulation, *International Journal of*  
568 *Impact Engineering*, 65 (2014) 79-88.
- 569 [13] C. Kılıçaslan, M. Güden, İ.K. Odacı, A. Taşdemirci, The impact responses and the finite  
570 element modeling of layered trapezoidal corrugated aluminum core and aluminum sheet  
571 interlayer sandwich structures, *Materials & Design*, 46 (2013) 121-133.
- 572 [14] L. St-Pierre, V.S. Deshpande, N.A. Fleck, The low velocity impact response of sandwich  
573 beams with a corrugated core or a Y-frame core, *International Journal of Mechanical Sciences*,  
574 91 (2015) 71-80.
- 575 [15] F. Côté, V.S. Deshpande, N.A. Fleck, A.G. Evans, The out-of-plane compressive behavior  
576 of metallic honeycombs, *Materials Science and Engineering: A*, 380 (2004) 272-280.
- 577 [16] C. Kılıçaslan, M. Güden, İ.K. Odacı, A. Taşdemirci, Experimental and numerical studies  
578 on the quasi-static and dynamic crushing responses of multi-layer trapezoidal aluminum  
579 corrugated sandwiches, *Thin-Walled Structures*, 78 (2014) 70-78.
- 580 [17] B.T. Cao, B. Hou, H. Zhao, Y.L. Li, J.G. Liu, On the influence of the property gradient  
581 on the impact behavior of graded multilayer sandwich with corrugated cores, *International*  
582 *Journal of Impact Engineering*, 113 (2018) 98-105.

- 583 [18] L.L. Yan, B. Yu, B. Han, C.Q. Chen, Q.C. Zhang, T.J. Lu, Compressive strength and  
584 energy absorption of sandwich panels with aluminum foam-filled corrugated cores,  
585 *Composites Science and Technology*, 86 (2013) 142-148.
- 586 [19] M. Yazici, J. Wright, D. Bertin, A. Shukla, Experimental and numerical study of foam  
587 filled corrugated core steel sandwich structures subjected to blast loading, *Composite*  
588 *Structures*, 110 (2014) 98-109.
- 589 [20] Y. Cheng, T. Zhou, H. Wang, Y. Li, J. Liu, P. Zhang, Numerical investigation on the  
590 dynamic response of foam-filled corrugated core sandwich panels subjected to air blast loading,  
591 *Journal of Sandwich Structures & Materials*, (2017) 109963621770035.
- 592 [21] L.L. Yan, B. Han, B. Yu, C.Q. Chen, Q.C. Zhang, T.J. Lu, Three-point bending of  
593 sandwich beams with aluminum foam-filled corrugated cores, *Materials & Design*, 60 (2014)  
594 510-519.
- 595 [22] H.N.G. Wadley, K.P. Dharmasena, M.R. O'Masta, J.J. Wetzel, Impact response of  
596 aluminum corrugated core sandwich panels, *International Journal of Impact Engineering*, 62  
597 (2013) 114-128.
- 598 [23] B. Han, K. Qin, B. Yu, B. Wang, Q. Zhang, T.J. Lu, Honeycomb–corrugation hybrid as a  
599 novel sandwich core for significantly enhanced compressive performance, *Materials & Design*,  
600 93 (2016) 271-282.
- 601 [24] R.-P. Yu, X. Wang, Q.-C. Zhang, L. Li, S.-Y. He, B. Han, C.-Y. Ni, Z.-Y. Zhao, T.J. Lu,  
602 Effects of sand filling on the dynamic response of corrugated core sandwich beams under foam  
603 projectile impact, *Composites Part B: Engineering*, (2020).
- 604 [25] X. Wang, R.-P. Yu, Q.-C. Zhang, L. Li, X. Li, Z.-Y. Zhao, B. Han, S.-Y. He, T.J. Lu,  
605 Dynamic response of clamped sandwich beams with fluid-filled corrugated cores,  
606 *International Journal of Impact Engineering*, 139 (2020).
- 607 [26] G.W. Kooistra, V. Deshpande, H.N. Wadley, Hierarchical corrugated core sandwich panel  
608 concepts, *Journal of applied mechanics*, 74 (2007) 259-268.
- 609 [27] L. Zhang, R. Hebert, J.T. Wright, A. Shukla, J.-H. Kim, Dynamic response of corrugated  
610 sandwich steel plates with graded cores, *International Journal of Impact Engineering*, 65 (2014)  
611 185-194.
- 612 [28] T. Zhao, Y. Jiang, Y. Zhu, Z. Wan, D. Xiao, Y. Li, H. Li, C. Wu, D. Fang, An experimental  
613 investigation on low-velocity impact response of a novel corrugated sandwiched composite  
614 structure, *Composite Structures*, 252 (2020).
- 615 [29] Z. Li, W. Chen, H. Hao, Q. Yang, R. Fang, Energy absorption of kirigami modified  
616 corrugated structure, *Thin-Walled Structures*, 154 (2020) 106829.
- 617 [30] X. Li, S. Li, Z. Wang, J. Yang, G. Wu, Response of aluminum corrugated sandwich panels  
618 under foam projectile impact – Experiment and numerical simulation, *Journal of Sandwich*  
619 *Structures & Materials*, 19 (2016) 595-615.